Proceedings of FBC2005
18th International Conference on Fluidized Bed Combustion
May 22-25, 2005, Toronto, Ontario, Canada

FBC2005-78070

STUDY ON POLLUTANTS EMISSION CHARACTERISTIC OF COAL GASIFICATION IN A FLUIDIZED BED TEST RIG

Zhaoping Zhong/Department of Power Engineering, The Key Laboratory of Clean Coal Power Generation and Combustion Technology of Ministry of Education, Southeast University, Nanjing, 210096, P. R. China

Baosheng Jin/Department of Power Engineering, The Key Laboratory of Clean Coal Power Generation and Combustion Technology of Ministry of Education, Southeast University, Nanjing, 210096, P. R. China

Yaji Huang/Department of Power Engineering, The Key Laboratory of Clean Coal Power Generation and Combustion Technology of Ministry of Education, Southeast University, Nanjing, 210096, P. R. China

Hongcang Zhou/Department of Power Engineering, The Key Laboratory of Clean Coal Power Generation and Combustion Technology of Ministry of Education, Southeast University, Nanjing, 210096, P. R. China

Davide Ross/ Graduate School of Bio-Applications and Systems Engineering (BASE), Tokyo University of Agriculture and Technology, Koganei, Tokyo 184-8588, Japan

Masayuki Horio/ Graduate School of Bio-Applications and Systems Engineering (BASE), Tokyo University of Agriculture and Technology, Koganei, Tokyo 184-8588, Japan

ABSTRACT

This paper presents the results of coal gasification in a fluidized bed test rig of Xuzhou bituminous coal. The diameter of the fluidized bed combustor is 0.1m and the height is 4.22m. The bed temperature is maintained by a method of high temperature flue gas interline heating to overcome high heat losses associated with a oil burner. Test results are reported for variations in the bed temperature, air to coal, steam to coal and Ca to S ratio and their influence on gas yields and desulphurization efficiency. The distribution of polycyclic aromatic hydrocarbons (PAHs) and heavy metal trace elements into the char and syngas are also presented.

The molar contents for CH_4 and H_2 in the coal syngas are found to decrease with increasing air to coal feed ratio from 2.5 to 5, while the content of CO shows little variation. Increasing the steam to coal feed ratio from 0.4 to 0.65 results in all three of the main gas components measured to form a local maximum content at a steam/coal feed ratio of 0.55. The efficiency of desulphurization improves as the ratio of Ca to S, air to coal and the bed temperature are increased, while decreasing with increasing steam to coal feed ratios. The volatile trace element species in decreasing order of relative mass ratio released into the gas phase are Hg, Se, As, Co, Cr, Cd, Cu, and Zn. Besides Hg, Se, and As, for all other trace heavy metals the majority of their mass distribution remains within the char with the proportion contained within char always greater than their combined yields in the coal syngas and slag. The total PAHs in the coal syngas is greater than that contained in the original coal and this indicates that PAHs are formed during the coal gasification process.

Keywords: coal, gasification, fluidized bed, desulphurization, trace element, PAHs

INTRODUCTION

Advanced Pressurized Fluidized Bed Combustion-Combined Cycle (APFBC-CC) is a promising technology for the cleaner and more efficient generation of electricity from coal. Coal partial gasification is a key step in the APFBC cycle. The majority of the sulphur present in coal changes into hydrogen sulfide under a reducing partial gasification atmosphere. At the same time, trace elements like As, Cd, Co, Cr, Cu, Mn, Mg, Ni, Hg, Pb, V, Se, Sr and Zn and PAHs in the coal gasification redistribute themselves into the slag, fly ash and coal gas phases.

Xiangling Hou [1] has carried out research to capture hydrogen sulfide at high temperature using ferric oxide micro particles. Yanxu Li [2] has studied the effect of oxygen atmosphere on desulphurization using ZnO and showed that the presence of O_2 will stifle the desulphurization reaction. Xueming Bu [3] has carried out research on gasification in a ϕ 100 I.D. pressurized fluidized bed using dolomite and limestone as a sulfur sorbent. Their results indicate: (1) The desulphurization efficiency improves as the molar ratio of Ca and S increases. (2) The influence of operation pressure on the desulphurization efficiency decided by the partial pressure of CO_2 and the operating temperature of the gasifier. (3) Dolomite and limestone can also remove sulfur from coal gasification, the increase of sulfur content in the coal can improve the desulphurization efficiency. Fu Zhao [4] observed that initially hydrogen sulfide is the main containing sulfur product and then changes greatly with the change of temperature. Laurent A. Fenouil (1995) [5] and S.Y. Lin (1996) [6] have studied desulphurization during coal partial gasification and oxidation of calcium oxide. Joseph J. Helble [7] have studied trace element

partitioning the during coal gasification process. The results show that for Illinois bituminous coal a significant mass fraction of each of elements As, Se, Sb, Pb, Hg vaporizes during gasification, where Cd, Cr, Co, Mo, Ni, U, and Th are relatively non-volatile. M. Diaz-Somoano [8] have studied trace element evaporation during coal gasification based on thermodynamic equilibrium calculation approach. Oriol Font[9] have studied speciation of major and selected trace elements in fly ash from Integrated Gasification Combined Cycle(IGCC) power plant. In the literature to date, there is limited data reported on the formation of PAHs, with the majority of work published for biomass gasification processes [10-13].

This paper presents the results for the influence of operation parameters on coal gasification and desulphurization, and the distribution of trace elements and PAHs during atmospheric coal gasification of a Chinese bituminous coal.

1. TEST RIG AND TEST MATERIAL

1.1 Test rig

Figure 1 shows the schematic of a fluidized bed gasifier test rig. The main components are as follows.

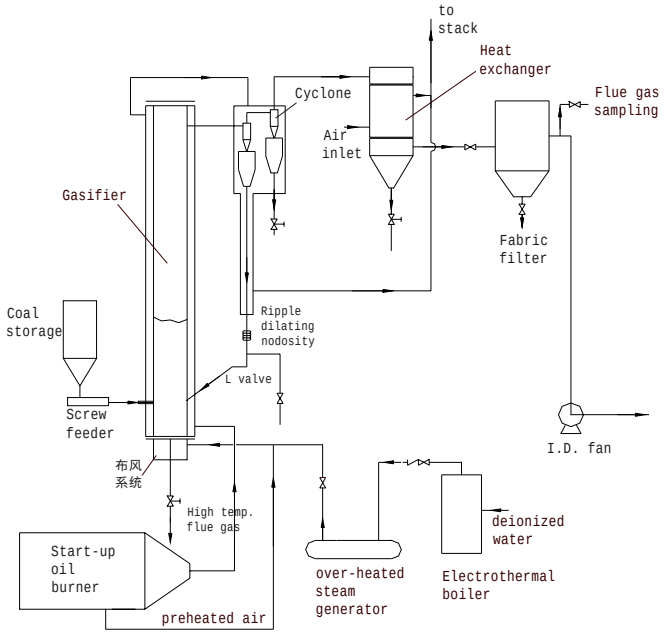

Figure 1. Schematic of fluidized bed gasifier test rig.

Table 1 Proximate and ultimate analyses of Xuzhou bituminous coal

C_{ar} (%)	H_{ar} (%)	O_{ar} (%)	N_{ar} (%)	S_{ar} (%)	V_{ar} (%)	Mar (%)	A_{ar} (%)	$Q_{net,ar}$ (MJ/kg)
70.40	4.54	7.86	1.24	0.63	30.57	2.72	12.62	28.91

Table 2 Analytical results of limestone and dolomite

	CaO	MgO	SiO_2	Al_2O_3	TiO_2	Fe_2O_3	K_2O	Na_2O	SO_3
Limestone	52.1	0.81	3.42	1.31	0.061	0.39	0.18	0.017	0.031
Dolomite	28.6	18.15				0.4			0.213

1.1.1 Heating system

This is composed of an oil tank, oil burner and a combustor. High-temperature flue gas at 850℃ emitted from the oil burner enters the interlining shell to heat the fluidized bed gasifier. At the same time, cold fluidizing air passes through a heat exchanger with the high-temperature flue gas to increase the temperature of the fluidized air.

1.1.2 Steam generation system

The steam generation system can be divided into two parts: galvanothermy boiler and over-heater steam generator. The rating steam temperature of galvanothermy boiler is 184 ℃. The temperature of the steam at the inlet and outlet of the over-heater steam generator are 175 ℃ and +400 ℃, respectively. The steam is then mixed with the preheated fluidizing air and then enters the fluidized bed gasifier through the air box and air distributor.

1.1.3 Feeding system

This is mainly composed of a electric motor, a reducer and a water cooled screw feeder. The end of the screw feeder lies within the high temperature zone.

1.1.4 Fluidized bed gasifier

This is composed of the inner-bed cylinder and the outer-shell. The size of inner-bed is Φ108×4mm, the height from air distributor to the inlet of cyclone is 4220 mm. The high temperature flue gas from the combustor enters the annulus between the bed and shell casing and in turn heats up the inner-bed and the primary and secondary cyclones before being discharged. The large particles removed by the primary cyclone are return to the bubbling bed through an ash recycle system.

1.2 Test material

Table 1 shows the proximate and ultimate analyses of the Xuzhou bituminous coal. The carbon content, volatile content and heating value of coal are high and ash content is low. The minimum fluidizing velocity for a 0.3 and 1.0 mm coal particle is 0.04 and 0.329 m/s respectively. The larger particle is difficult to fluidize and the small particle has a short residence time in the fluidized bed which is disadvantageous for gasification. The average particle size of coal adopted in the experiment was 0.9 mm and ranged in size between 0.2 mm to 1.4 mm. The sulfur sorbents used in the experiments are limestone and dolomite from Nanjing with the component analyses shown in Table 2. The size of the sulfur sorbents ranged between 0.2 to 1.0 mm.

1.3 Measurement

The main measurement parameters recorded are the temperature, pressure, flow rates of air and steam and the product gas concentrations, CO, CO_2, CH_4, H_2, N_2 which are measured by a 1102-type gas chromatographic apparatus. The measurement of H_2S in the syngas is by a chemical iodine testing method. As seen from figure 2, a modified USEPA Method 5 is used for trace element sampling of the gas. The

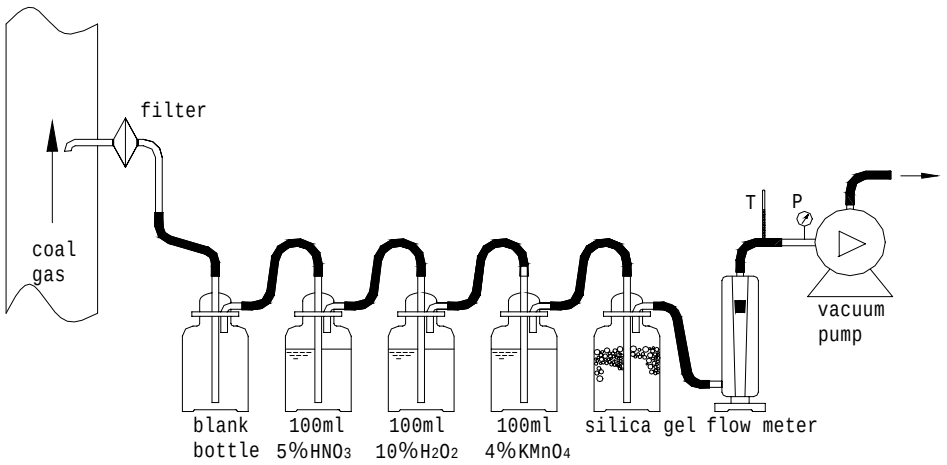

Figure 2 Gas sampling for trace elements

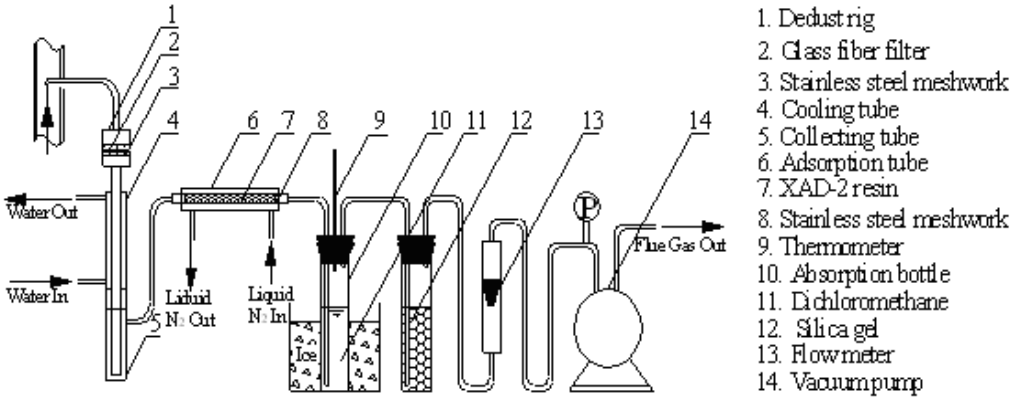

Figure 3 The sampling train for PAH in syngas

first blank bottle acts as a buffer. The second and third bottles are used to absorb the trace elements except for Hg. The fourth bottle absorbs the Hg in coal gas. The last bottle is a dry bottle. The sampling point is after the fabric filter. 14 trace elements are measured and these are; As, Cd, Co, Cr, Cu, Mn, Mg, Ni, Hg, Pb, V, Se, Sr, Zn. A hydride generator and atom fluorescence spectrum method (HG-AFS) are used to measure Hg, As, Se. The other trace elements are measured by use of the Inductively Coupled Plasma Atomic Emission Spectrometry (ICP-AES).

The sampling train for PAH in syngas is shown in figure 3. The syngas containing PAHs is sampled using a stainless sampling probe and passes through a glass fiber filter to remove the fine particles. It then passes through a water cooling tube to condensed the light molecular weight PAHs with the remaining PAHs captured using an adsorption tube packed with 5 g XAD-2 resin and an absorption bottle filled with dichloromethane. All samples containing PAHs were refrigerated at 4 ^{o}C before their extraction.

The collected samples containing the PAHs are first extracted for 8 h by Soxhlet extraction. Then, the concentrated solution is made to pass through a purifying tube packed with activated silica gel. The purifying tube is then eluted to obtain PAHs in the purifying solution. Further, the purified solution is condensed to 1 ml by using a K-D concentrator and a gentle stream of pure nitrogen. Finally, the extracted samples are placed into brown vials and stored at 4 ^{o}C for analysis.

The samples are analyzed by the Waters Alliance HPLC system coupled with a Waters 2695 Separations Module, a Waters 2475 Multi λ Fluorescence Detector, and a Waters 2996 PDA Detector. Injections of 1 µl samples were made onto a C18 column (length 250 mm, 4.6 mm i.d.) containing 5 µm particles for PAHs. The mobile phase, flowing at 1.2 ml/min, is programmed to hold, followed by an 11 min ramp to a composition of 100% of acetonitrile, and finally a mixture of 60:40 (v/v, %) acetonitrile and water for 7 min. The excitation and emission wavelength of the fluorescence detector are 224 nm and 330 nm, respectively. The wavelength of PDA detector is 254 nm. The concentrations of the 16 PAHs recommended by US EPA are determined from naphthalene to indeno(1,2,3-cd)pyrene. The HPLC is calibrated with a diluted standard solution of 16 PAH compounds (PAH Mixture-610M from Supleco) recommended by the US EPA. The recovery efficiencies of the 16 PAH compounds ranged from 60% to 117%, and the method detection limit (MDL) ranged from 1.92pg to 233 pg.

2. TEST RESULTS AND ANALYSIS

2.1 Definition of terms

Desulphurization efficiency = outlet concentration of H_2S with sulfur sorbent addition / outlet concentration of H_2S with no sulfur sorbent addition.

Air to coal ratio = mass of air / mass of coal.

Steam to coal ratio = mass of steam / mass of coal.

Mass equilibrium ratio of trace elements = the total mass of trace elements per unite time after gasification / mass of trace elements in coal per unite time.

2.2 The influence of air to coal ratio on experimental results

The influence of air to coal ratio on the experimental

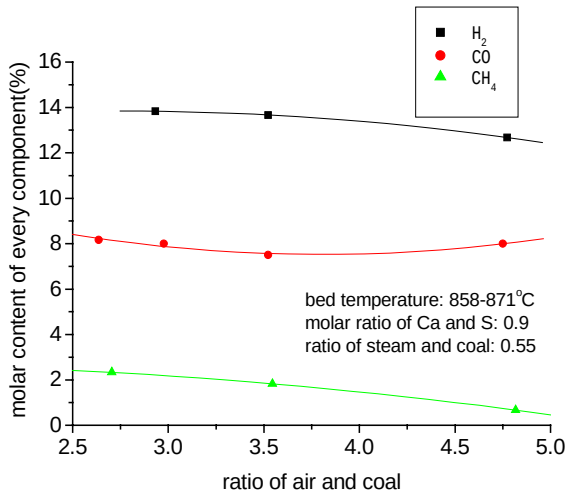

Figure 4 The influence of ratio of air and coal on molar content of syngas

results is shown in Figures 4 and 5. From Figure 4 we can see that the content of CH_4 and H_2 decrease gradually with the increase in air to coal ratio. With the comparative increase of fluidizing air, the total gas quantity at the exit will increase and the absolute content of N_2 (major component) will also increase. Therefore the comparative contents of CH_4 and H_2 will decrease.

With the improvement of oxygen atmosphere and the rising bed temperature, the higher content of CO_2 will lead to the rate of the reducing reaction being enhanced increasing the CO concentration.

For CO and H_2 there are two competing aspects that must be considered. With the increase in air to coal feed ratio there is a co-current rise in bed temperature, consequently the steam gasification reaction rate of carbon increases to produce more CO and H_2. However, with the increase of O_2 in the bed, there is also an increase in competition between heterogeneous and homogeneous reactions for the available O_2, resulting in combustion loss in the gas phase [14].

Figure 5 shows the relationship between the air to coal feed ratio and desulphurization efficiency. In the range of experiment, the desulphurization efficiency increases with the increase in air to coal feed ratio. This causes a rise in the bed temperature and higher temperatures favor the gasification and desulphurization reactions [15].

2.3 The influence of steam to coal ratio

From figure 6 and 7, we can see that the influence of ratio of steam and coal on experimental results. It can be seen in figure 6 that H_2 get from the reaction will increase with the comparative increase of steam flux obviously. After the ratio of steam and coal greater than 0.55, the molar content of H_2 in syngas will decrease a little.

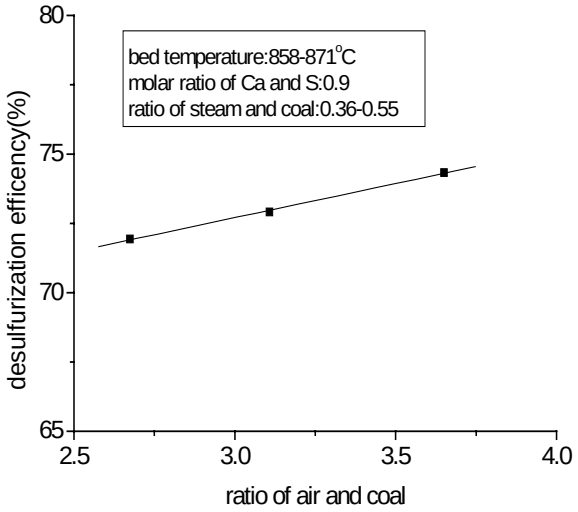

Figure 5 The influence of air to coal ratio on desulphurization efficiency

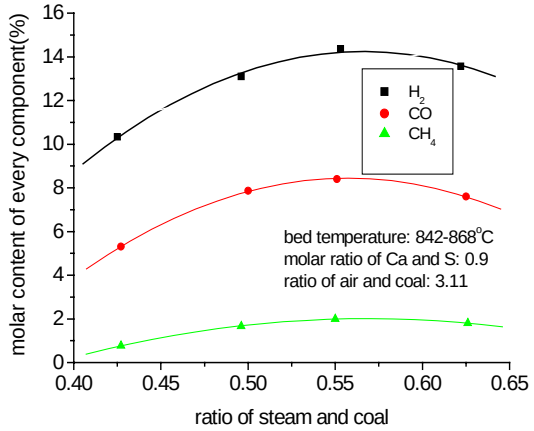

Figure 6 The influence of steam to coal ratio on molar content of syngas

In addition the decrease of the bed temperature is detrimental to the gasification reaction rate and lowers the H_2 content. The trend of CH_4 increases at first because of the increase of content of H_2 and CO in the gas component leads to the quantitative increase of CH_4 and the decrease at last is also influenced by the decrease of H_2 flux. CO increases quickly at the initial phase because the flux that is produced through direct reaction is more. Moreover at first the quick increase of CO leads the reaction of CO and steam move to the positive direction. It will decrease the CO content in total gas flux.

The relationship between the steam to coal feed ratio and desulphurization efficiency can be seen in Figure 7. The desulphurization efficiency decreases with increasing steam to coal feed ratio because this leads to a decrease in the bed temperature and temperature is one of the main factors that influence desulphurization efficiency [15]. Additionally, by increasing the steam concentration the balance for the desulphurization reaction between H_2S and CaO which is a reversible reaction, changes the equilibrium favoring the

reverse of the desulphurization reaction and thus more H_2S remains unconverted and desulphurization efficiency decreases.

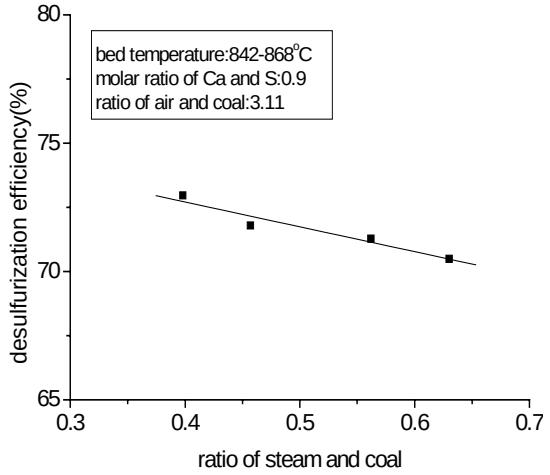

Figure 7 The influence of ratio of steam and coal on desulphurization efficiency

2.4 The influence of other factors on desulphurization efficiency

From Figure 8, it can be seen that desulphurization efficiency gradually increases with an increase in the molar ratio between Ca and S. In this experiment the main desulphurization reaction is $CaO+H_2S \rightarrow CaS+H_2O$ − 68.49kj/mol. It can be deduced that the equilibrium partial pressure of CO_2 in this experiment is between 0.4 atm and 0.8 atm from the equilibrium partial pressure formula of CO_2 during the $CaCO_3$ decomposition, that is $\lg\left(P_{CO_2}\right) = -8799.7/T_k + 7.521$.

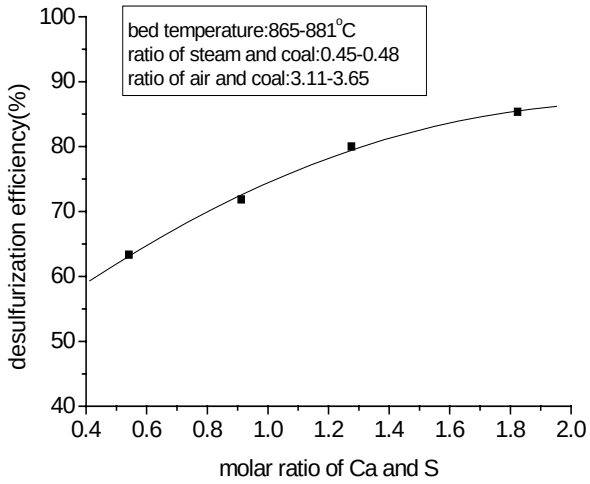

Figure 8 The influence of molar ratio of Ca and S on desulphurization efficiency

The calculated equilibrium partial pressure of CO_2 is larger than the partial pressure of CO_2 in the furnace. This shows that desulphurization reaction lies in the calcining zone of sulphur sorbent and $CaCO_3$ decomposes into CaO. A rise in the molar ratio of Ca to S improves the concentration of CaO present in the gasifier to reduce H_2S and thus improving the desulphurization efficiency. The influence of temperature on desulphurization efficiency can be seen from Figure 9.

At a given molar ratio of Ca to S, a rise in temperature increases favors the desulphurization reaction and makes it easy to reach the equilibrium state and desulphurization efficiency is improved overall.

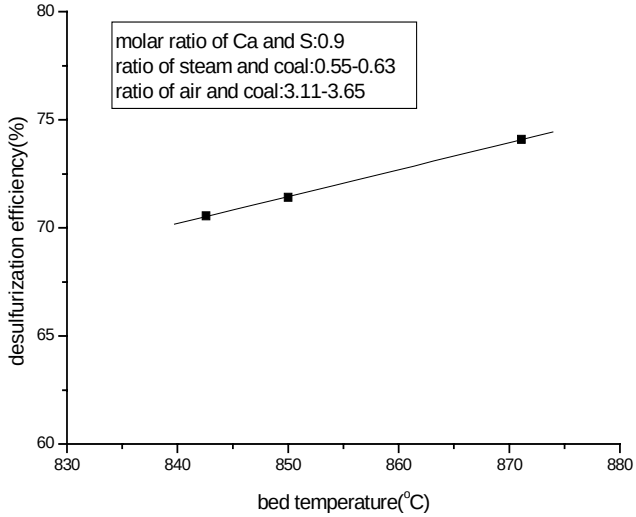

Figure 9 The influence of bed temperature on desulfurization efficiency

Figure 10 shows the influence of two different kinds of sulfur sorbents on desulphurization efficiency. Sulfur sorbents such as dolomite and limestone can capture H_2S produced from coal gasification. Typically, dolomite contains more $MgCO_3$ then in limestone resulting in higher particle porosity as dolomite calcinates to MgO. This normally improves the

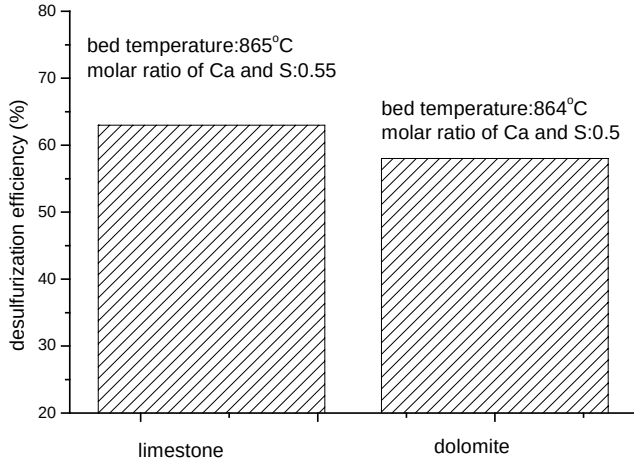

Figure 10 The comparison of desulphurization using limestone and dolomite

desulphurization capability but the present data does not support this. The desulphurization reaction using CaO to remove H_2S has not pore block phenomena [15]. But calcined $MgCO_3$ produces CO_2 which can produce inter-particle pressures resulting in particle fracture and disintegration. This results in the formation of dolomite fine particles that entrain out of the bed before reaction and desulphurization can occur.

Therefore the consumption rate of dolomite will be more than for limestone at the same molar ratio of Ca to S and therefore results in higher operating costs for the desulphurization process.

2.5 The distribution of trace elements during coal gasification

As seen in Figure 11, the mass equilibrium ratio of As, Hg, V, Se is 75～83%, the mass equilibrium ratio of Co, Cr, Cu, Pb, Sr, Zn is 88～105%, the mass equilibrium ratio of Cd, Mn, Mg, Ni is 115～118%. For the more volatile elements, condensation on pipe walls additionally to the general sampling and analysis error are main reasons for the differences in mass balances. In decreasing order of concentration in the coal syngas the following elements are detected as shown in Figure 11, Hg, Se, As, Co, Cr, Cd, Cu and Zn. Hg, Se and As are the most volatile elements and this accounts for their relative high numbers. The bottom slag contains Se and As. One reason for this is that Se and As can react with Ca compounds to form products such as $Ca_3(AsO_4)_2$ and CaSe which are stable non-volatle compounds. High and low temperature chars both absorb Hg from the gas phase.

2.6 PAHs of the coal gasification process

The concentrations of 16 US EPA specified PAH species were determined by high performance liquid chromatography (HPLC), including naphthalene (NaP), acenaphthylene (AcPy),

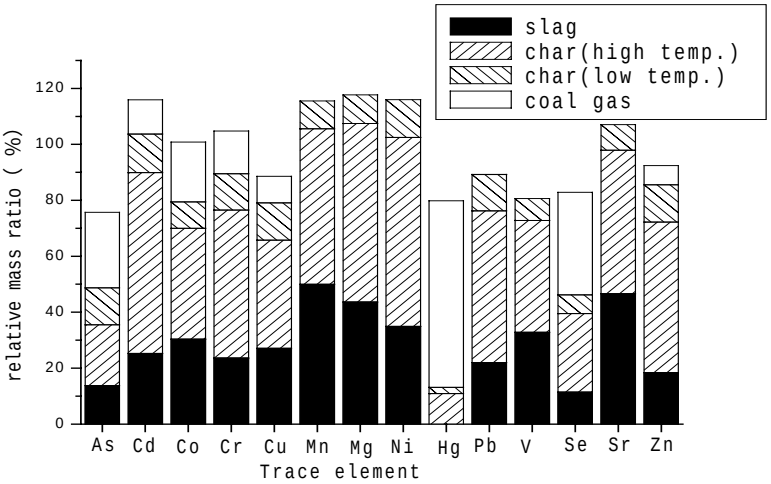

Figure 11 The distribution of trace elements in coal gasification
(Bed temperature: 920～945℃, steam to coal ratio: 0.43kg/kg, Air to coal ratio: 2.7Nm^3/kg)

Table 3 PAHs of the coal gasification process
(bed temperature: 920～945℃, ratio of steam and coal: 0.43kg/kg, ratio of air and coal: 2.7Nm^3/kg)

		Coal		Char(bag filter ash)		Syngas	
		mg·kg^{-1}	mg ·kg^{-1} (TEQ)	mg·kg^{-1}	mg ·kg^{-1} (TEQ)	μg·Nm^{-3}	μg ·Nm^{-3} (TEQ)
P A H	NaP	2.25	0.00225	3.66	0.00366	321.31	0.32131
	AcP	0.14	0.00014	0.00	0.00000	1373.47	1.37347
	AcPy	0.00	0.00000	12.53	0.01253	167.94	0.16791
	Flu	0.33	0.00033	12.87	0.01287	53.88	0.05388
	PhA	2.04	0.00204	96.87	0.09687	213.13	0.21313
	AnT	0.43	0.00430	57.17	0.57170	101.1	1.01100
	FluA	5.11	0.00511	153.51	0.15351	315.79	0.31579
	Pyr	0.91	0.00091	205.37	0.20537	336.81	0.33681
	Chr	5.39	0.05390	85.58	0.85580	160.63	1.60630
	BaA	1.40	0.14000	22.40	2.24000	41.83	4.18300
	BbF	0.78	0.07800	31.52	3.15200	50.28	5.02800
	BkF	0.00	0.00000	8.36	0.83600	39.81	3.98100
	BaP	0.47	0.47000	63.08	63.08000	72.60	72.60000
	DbA	0.00	0.00000	34.81	34.81000	33.43	34.43000
	In(123-cd)P	0.00	0.00000	7.74	0.77400	12.51	1.25100
	BghiP	0.00	0.00000	14.06	0.14060	7.88	0.07880
Ring	2R	1.91		3.66		321.31	
	3R	3.82		179.45		1909.51	
	4R	13.44		466.87		855.05	
	5R	1.25		137.77		196.12	
	6R	0.00		21.08		20.39	
Total		20.42	0.75698	809.55	106.94491	3302.39	125.95140

acenaphthene (AcP), fluorene (Flu), phenanthrene (PhA), anthracene (AnT), fluoranthene (FluA), pyrene (Pyr), benzo(a)anthracene (BaA), chrysene (Chr), benzo(b)fluoranthene (BbF), benzo(k)fluoranthene (BkF), benzo(a)pyrene (BaP), indeno(1,2,3,-cd)pyrene (In(1,2,3-cd)P), dibenzo(a,h)anthracene (DbA) and benzo(ghi)perylene (BghiP).

Table 3 lists the PAH concentration of raw coal, char (bag filter ash) and coal syngas. Very little PAHs are detected in the slag. As seen in Table 3, the total PAHs concentration of raw coal and char are 20.42mg/kg and 809.55mg/kg, respectively. PAHs in the coal syngas is 3302.39μg/Nm^3. Therefore, the highest concentration of PAHs detected is in the char. One reason for is that char has a large adsorption capacity because of its large surface area. Another reason is PAHs vapor easily condense into the solid state at lower temperature.

In this experiment, raw coal and coal syngas are dominated by three- and four-ringed PAHs, but char is dominated by three- to five-ringed PAHs. Material balance calculations indicated partial PAHs are formed in the coal gasification process. This is because PAHs can be produced form thermal decomposition at high temperatures and small molecule catalyzed synthesis under the coal gasification process.

Perng-Jy Tsai et al.[16] used the Toxic Equivalent Factor (TEF) to assess the harm of different PAH to human health from a health-risk assessment view point. The toxicity of PAH is expressed as TEF in relation to the most toxic PAH. The TEFs for the 16 PAHs specified by US EPA have been determined by Perng-Jy Tsai et al. In this study, the concentration of each PAH species is converted to the toxic equivalent (TEQ) concentration and is shown in Table 3. The total TEQ concentration of PAHs in char is greater than that of raw coal. It means some high toxic equivalent value of PAHs such as BaP and DbA are formed during the coal gasification process.

3. CONCLUSIONS

The molar contents for CH_4 and H_2 in the coal syngas are found to decrease with increasing air to coal feed ratio from 2.5 to 5, while the content of CO shows little variation. Increasing the steam to coal feed ratio from 0.4 to 0.65 results in all three of the main gas components measured increasing to form a local maximum in molar content at a steam/coal feed ratio of 0.55. The desulphurization efficiency increases with an increase in the air to coal ratio and a decrease in the steam to coal, respectively. Limestone and dolomite have relatively similar desulphurization efficiencies but the consumption of dolomite is higher possibly due to higher rates of entrainment. So limestone should be selected as sulfur sorbent for desulphurization during atmospheric coal gasification. The efficiency of desulphurization improves as the molar ratio of Ca to S and bed temperature is increased. The volatile trace element species in decreasing order of relative mass ratio released into the gas phase are Hg, Se, As, Co, Cr, Cd, Cu, and Zn. Besides Hg, Se and As, other trace elements concentration in the char are greater than the combined values found in the coal syngas and slag. PAHs in coal are dominated by three-, and four-ringed PAHs. The total PAH in coal gasification products is greater than that in the raw coal. Some high toxic equivalent value of PAHs can be formed in the coal gas gasification process.

ACKNOWLEDGMENTS

Authors would like to acknowledge support received for this paper from the state key basic research program of the Ministry of Science and Technology of China (G19990221053), the excellent young teacher of universities by the State Education Ministry of China, and key project funds for science and technology research by the State Education Ministry of China.

REFERENCES

[1] Xianglin Hou et.al. The research on using Fe_2O_3 small particles to get rid of H_2S at high temperature, Environmental Science, 1996, Vol.17(4)

[2] Yanxu Li et.al. The oxygen aural offect and kinetic token during desulfurization using ZnO, Fuel chemistry transaction, 1996, Vol.24(1): 18-24

[3] Xuepeng Bu et.al. The research on desulfurization that coal is gasified in fluidizing bed, Environmental engineering, 1996, Vol.17(2): 39-41

[4] Fu Zhao et.al. The research on release of gaseous contamination under the condition that coal is gasified and steam is used to fluidize, Environmental science transaction, 1998,Vol.18(3): 225-229

[5] Laurent A.Fenouil and Scott Lynn. Study of Calcium-Based Sorbents for High-Temperature H_2S Removal.3.Comparison of Calcium-Based Sorbents for Coal Gas Desulfurization. Int.Eng.Chem.Res., 1995, Vol.34: 2343-2348

[6] S.Y.Lin,H.Matsuda and M.Husatani. Desulfurization in coal partial gasification/combustion bombined cycle. The 5th Int.conf.on CFB, 1996, CSNA3, pp.1-6

[7] Joseph J. Helble, Wahab Mojtahedi, Jussi Lyyranen, et al. Trace element partitioning during coal gasification, 1999,

[8] M. Diaz-Somoano, M. R. Martinez-Tarazona. Trace element evaporation during coal gasification based on a thermodynamic equilibrium calculation approach, FUEL, 2003, Vol. 82, 137-145

[9] Oriol Font, Xavier Querol, Frank E. Huggins, et al. Speciation of major and selected trace elements in IGCC fly ash, Fuel, Available online 13 December, 2004

[10] O. Moersch, H. Spliethoff, K. R. G. Hein. Tar quantification with a new online analyzing method, Biomass and Bioenergy, 2000, Vol. 18, 79-86

[11] C. M. Kinoshita, Y. Wang, J. Zhou. Tar formation under different biomass gasification conditions, Journal of Applied Pyrolysis, 1994, Vol. 29, 169-181

[12] Pia Oesch, Eero Leppamaki, Pekka Stahlberg. Sampling and characterization of high-molecular-weight polyaromatic tar compounds formed in the pressurized fluidized-bed gasification of biomass, FUEL, 1996, 75(12), 1406-1412

[13] Philipp Morf, Philipp Hasler, Thomas Nussbaumer. Mechanisms and kinetics of homogeneous secondary reactions of tar from continuous pyrolysis of wood chips, FUEL, 2002, Vol. 81, 843-853

[14] Ross, D.P, Yan, H.M. and Zhang, D.K. Modeling of a laboratory-scale bubbling fluidized-bed gasifier with feeds of both char and propane, *Fuel*, 2004, 83 (14/15), 1979-1990

[15] Zhaoping Zhong, Jixiang Lan, Baosheng Jin, et al. Research on kinectics of limestone desulfurization reaction under a reducing atmosphere, International Journal of Energy Research, 1999, Vol. 23, 207-215

[16] Tsai, P.J., Shieh, H.Y., Lee, W.J., Lai S.O. Characterization of PAHs in the atmosphere of carbon black manufacturing workplaces. *J. Hazard. Mater.* 2002, A91, 25-42